Chapter 6

Vibrational Study and Crystal Structure of Barium Cesium Cyclotriphosphate Dihydrate

Soufiane Zerraf, Mustafa Belhabra,
Aziz Kheireddine, Malika Tridane,
Hicham Moutaabbid, Mohammed Moutaabbid and
Said Belaaouad

Additional information is available at the end of the chapter

http://dx.doi.org/10.5772/intechopen.81118

Abstract

Chemical preparation, crystal structure, thermal behavior, and IR studies are reported for the barium cesium cyclotriphosphate dihydrate $BaCsP_3O_9.2H_2O$ and its anhydrous form $BaCs_4(PO_3)_6$. $BaCsP_3O_9.2H_2O$, isotypic to $BaTlP_3O_9.2H_2O$ and $BaNH_4P_3O_9.2H_2O$, is monoclinic P21/n with the following unit cell dimensions: a = 7.6992(2)Å, b = 12.3237(3)Å, c = 11.8023(3)Å, α = 90 (2)°, β = 101.18(5)°, γ = 90. (3)°, and Z = 4. The total dehydration of $BaCsP_3O_9.2H_2O$ is between 100°C and 580°C. The IR absorption spectroscopy spectrum for the crystal confirms that most of the vibrational modes are comparable to similar cyclotriphosphates and to the calculated frequencies. The thermal properties reveal that the compound is stable until 90°C.

Keywords: barium cesium cyclotriphosphate, crystal structure, vibrational study

1. Introduction

During a systematic investigation of cyclophosphates, types $BaCsP_3O_9.xH_2O$, $BaCs_4(P_3O_9)_2.xH_2O$, $BaCs_2P_4O_{12}.2H_2O$, $Ba_3Cs_2(P_4O_{12})_2.2H_2O$, and $BaCsP_3O_9.2H_2O$ were obtained. Barium and cesium cyclotriphosphate dihydrate, $BaCsP_3O_9.2H_2O$, was prepared for the first time by using Boulle's process [1] by Masse and Averbuch-Pouchot [2], who described it as a monohydrate. The literature provides $BaCsP_3O_9.2H_2O$ crystallizing in the monoclinic system, space group $P2_1/n$, Z = 4 with the following unit cell parameters, $a = 7.6992(2)$ Å, $b = 12.3237(3)$ Å, *c = 11.8023 (3)* Å, and *β = 101.181 (5)°* with a brief report of the structural refinement based on single-crystal XRD data. In the present work, we report the chemical preparation, crystalline structure, thermogravimetric analysis, and infrared study of this crystal barium and cesium cyclotriphosphate dihydrate, $BaCsP_3O_9.2H_2O$, in order to have maximum information about structure and reactivity of the solids.

2. Experimental parameters

2.1. Chemical preparation

Single crystals of $BaCsP_3O_9.2H_2O$ were prepared by slowly adding dilute cyclotriphosphoric acid, $H_3P_3O_9$, to an aqueous solution of barium carbonate, $BaCO_3$, and cesium carbonate, Cs_2CO_3, with a stoichiometric ratio of Ba-Cs = 1:1, according to the following chemical reaction:

$$H_3P_3O_9 + BaCO_3 + 1/2Cs_2CO_3 \longrightarrow BaCsP_3O_9.2H_2O + 3/2CO_2$$

The solution was then slowly evaporated at room temperature for 45 days until single crystals of $BaCsP_3O_9.2H_2O$ were obtained. The cyclotriphosphoric acid, $H_3P_3O_9$, used in this reaction was prepared from an aqueous solution of $Na_3P_3O_9$ passed through an ion-exchange resin "Amberlite IR120" [3]. $Na_3P_3O_9$ was obtained by thermal treatment of sodium dihydrogen monophosphate, NaH_2PO_4, at 530°C for 5 h in the air, according to the following chemical reaction [4]:

$$3NaH_2PO_4 \longrightarrow Na_3P_3O_9 + 3H_2O$$

2.2. XRD, crystal data, intensity data collection, and structure

A single-crystal X-ray structure determination of $BaCsP_3O_9.2H_2O$ was performed by using an Oxford Xcalibur S diffractometer at 293 K.

The structure was solved by direct methods using SHELXS [5] implemented in the Olex2 program [6]. The refinement was then carried out with SHELXL by full-matrix least squares minimization and difference Fourier methods. All non-hydrogen atoms were refined with anisotropic displacement parameters. Hydrogen atoms were generated in idealized positions, riding on the carrier atoms, with isotropic thermal parameters.

The final R1 value is 0.0401 for 1782 reflections with $I > 2\sigma(I)$, and full X-crystal data is presented in **Table 1**. The main geometrical features, bond distances, and angles are reported in **Table 6**.

2.3. Fourier transform infrared spectroscopy (FTIR)

A Nicolet Magna IR 560 spectrometer (resolution 1 cm^{-1}, 200 scans) and an OMNIC software were used to characterize the stretching and bending bands between 400 and 4000 cm^{-1}.

Compound	2
Empirical formula	BaCs $H_4O_{11}P_3$
Formula weight	543.20 g.mol^{-1}
Crystal system/space group	Monoclinic/$P\ 2_1/n$
a/Å	7.6992(2) Å
b/Å	12.3237(3) Å
c/Å	11.8023(3) Å
α/°	90°
β/°	101.18(3)°
γ/°	90°
V/Å^3	1098.57(5)Å^3
Z	4
D_{calc} (g/cm^3)	3.284 g/cm^3
μ (mm^{-1})	7.362
Crystal size (mm)	0.3296 × 0.1602 × 0.0957 mm^3
Color/shape	Colorless/prism
Temp (K)	293(2)K
Theta range for collection	3.50°/27.59°
Reflections collected	9176
Independent reflections	2448
Data/restraints/parameters	2448/0/147
Goodness of fit on F^2	1.113
Final R indices [I > 2σ(I)]	R_1 = 0.0285, wR_2 = 0.0611
R indices (all data)	R_1 = 0.0329, wR_2 = 0.0638
Largest difference peak/hole	0.78/−1.40 Å^{-3}

Table 1. Crystal data and experimental parameters for the X-ray intensity data collection for $BaCsP_3O_9.2H_2O$.

3. Results and discussion

3.1. Structural analysis

The final atomic positions and anisotropic thermal parameters for the non-hydrogen atoms in the $BaCsP_3O_9.2H_2O$ structure are given in **Tables 2** and **3**, respectively. A projection of the $BaCsP_3O_9.2H_2O$ atomic arrangement along the c axis is given in **Figure 1**. It shows that all the components of the atomic arrangements are located around the two axes in order to form arrays delimiting large channels parallel to the c direction.

Atoms	X	Y	Z	U_{eq}
Ba	0.24946(3)	0.06963(2)	0.37463(2)	0.01486(9)
Cs	1.23531(4)	0.37670(3)	0.60501(3)	0.02500(10)
P(1)	0.49653(15)	0.33939(9)	0.34729(10)	0.0135(2)
P(2)	0.75498(15)	0.17362(10)	0.42595(10)	0.0140(2)
P(3)	0.72984(16)	0.35936(10)	0.57392(11)	0.0185(3)
O(1i)	0.8311(4)	0.2619(3)	0.5238(3)	0.0194(7)
O(2i)	0.6424(4)	0.2510(2)	0.3278(2)	0.0159(7)
O(3i)	0.6022(4)	0.4024(2)	0.4588(3)	0.0178(7)
O(4e)	0.8606(5)	0.4456(3)	0.6136(4)	0.0393(10)
O(5e)	0.6256(5)	0.3191(3)	0.6572(3)	0.0312(9)
O(6e)	0.4740(4)	0.4168(2)	0.2497(3)	0.0212(7)
O(7e)	0.9053(4)	0.1308(3)	0.3805(3)	0.0223(8)
O(8e)	0.6306(4)	0.0994(3)	0.4691(3)	0.0201(7)
O(9e)	0.3428(4)	0.2843(3)	0.3783(3)	0.0205(7)
O(10w)	0.2195(4)	0.1274(3)	0.5953(3)	0.0233(8)
O(11w)	0.5532(5)	0.0975(3)	0.7172(3)	0.0315(9)
H(1)	0.5738	0.0941	0.7926	0.047
H(2)	0.5846	0.1617	0.6363	0.047
H(3)	0.1274	0.1017	0.6242	0.035
H(4)	0.3191	0.0980	0.6366	0.035

i, internal; e, external; w, water.

Table 2. Final atomic coordinates and U-equivalent temperature factors for $BaCsP_3O_9.2H_2O$.

3.2. Barium and cesium arrangement in the structure

The barium atom, located on the twofold axis, is coordinated by two water molecules and six oxygen atoms (**Figure 2**), forming an almost regular dodecahedron. The Ba-O distances spread between 2.298(6) and 2.349(6) Å. Each BaO_8 dodecahedron shares six oxygen atoms with two anionic rings belonging to two phosphoric layers, thus providing the cohesion between these layers (**Figure 2**). BaO_8 dodecahedra do not share any edge or corner and form layers alternating with P_3O_9 ones. The shortest Ba-Ba distance is found to be 4.70731 Å (**Table 4**).

The cesium atom occupies a general position and is coordinated to 10 external oxygen atoms and one water molecule (**Figure 3**). The Cs-O distances spread between 3.0278(2) and 3.5982(9) Ǻ.

The water group, its environment, established by strong hydrogen bonds, is depicted in (**Figure 3**) as an ORTEP representation [7].

Atom	U11(s)	U22	U33	U23	U13	U12
Ba	0.01483(15)	0.01281(16)	0.01595(15)	0.00044(10)	0.00056(11)	−0.00029(10)
Cs	0.02411(18)	0.0258(2)	0.02600(18)	0.00406(13)	0.00715(14)	0.00042(13)
P(1)	0.0146(6)	0.0132(6)	0.0122(5)	0.0016(4)	0.0015(5)	0.0020(5)
P(2)	0.0150(6)	0.0130(6)	0.0134(5)	0.0004(5)	0.0016(5)	0.0028(5)
P(3)	0.0171(6)	0.0193(7)	0.0171(6)	−0.0062(5)	−0.0015(5)	0.0022(5)
O(1i)	0.0173(16)	0.0172(17)	0.0207(17)	−0.0054(14)	−0.0035(14)	0.0032(14)
O(2i)	0.0195(17)	0.0166(17)	0.0113(15)	0.0007(13)	0.0023(13)	0.0071(14)
O(3i)	0.0192(17)	0.0140(17)	0.0176(17)	−0.0035(13)	−0.0026(14)	0.0027(14)
O(4e)	0.025(2)	0.027(2)	0.058(3)	−0.0226(19)	−0.0086(19)	−0.0009(17)
O(5e)	0.037(2)	0.037(2)	0.0201(18)	0.0038(16)	0.0079(17)	0.0101(18)
O(6e)	0.0241(18)	0.0194(17)	0.0210(18)	0.0080(14)	0.0067(15)	0.0069(15)
O(7e)	0.0173(17)	0.0245(19)	0.0247(18)	−0.0051(15)	0.0031(15)	0.0064(14)
O(8e)	0.0201(17)	0.0147(17)	0.0253(18)	0.0064(14)	0.0042(15)	0.0009(14)
O(9e)	0.0177(17)	0.0185(18)	0.0255(18)	0.0026(14)	0.0050(15)	−0.0004(14)
O(10w)	0.0190(17)	0.027(2)	0.0236(18)	−0.0012(15)	0.0043(15)	0.0010(15)
O(11w)	0.030(2)	0.034(2)	0.028(2)	−0.0008(17)	−0.0009(18)	−0.0001(18)

i, internal; e, external; w, water.

Table 3. Anisotropic thermal parameters (Å^2) for $BaCsP_3O_9.2H_2O$.

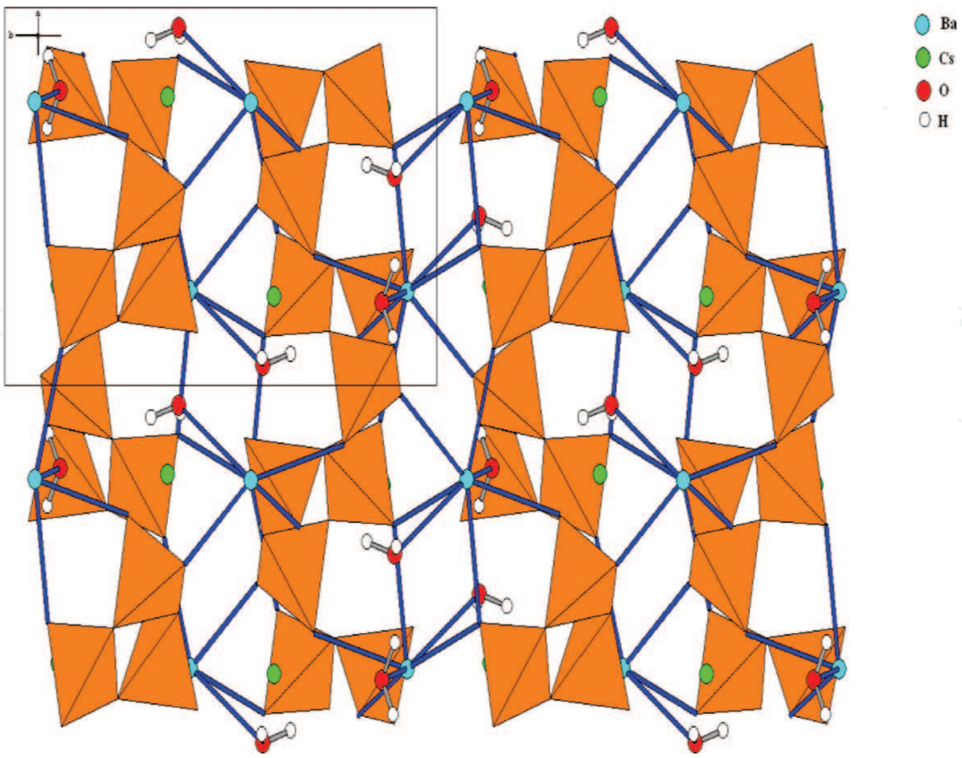

Figure 1. Projection along the c axis of the atomic arrangement in $BaCsP_3O_9.2H_2O$.

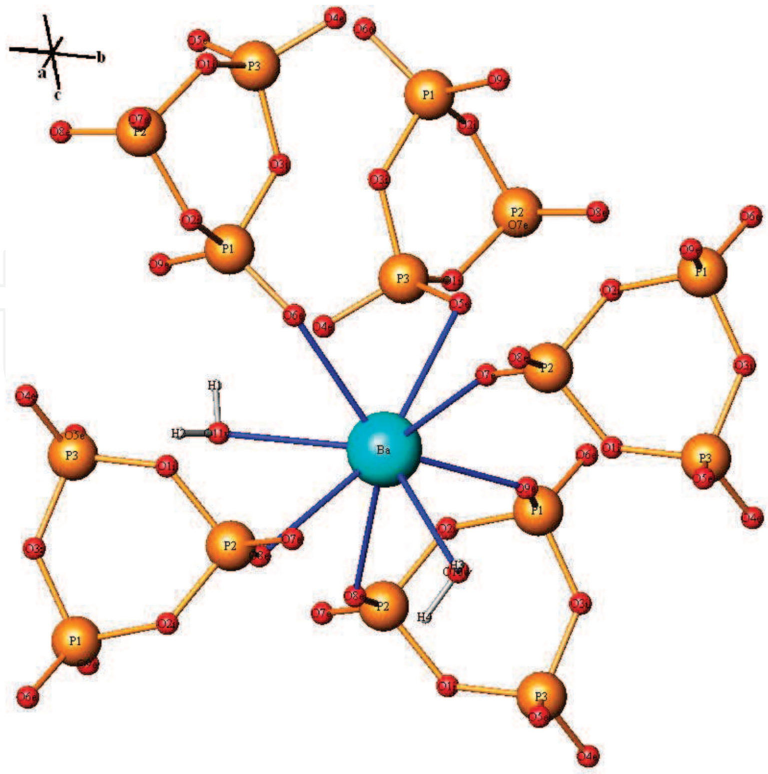

Figure 2. The coordination of the barium atom in $BaCsP_3O_9.2H_2O$.

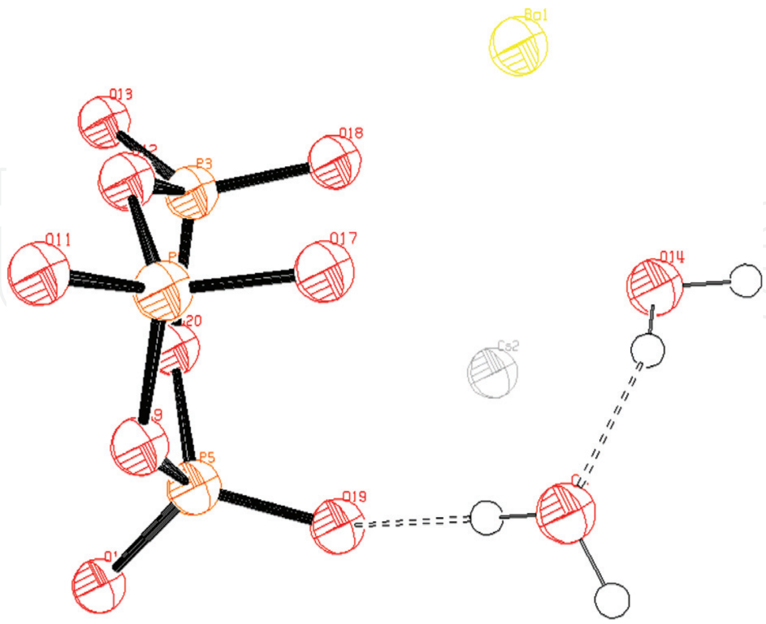

Figure 3. ORTEP representation of $BaCsP_3O_9.2H_2O$ (H-bonds are represented by dashed lines). Thermal ellipsoids are scaled to enclose 50% probability.

Tetrahedron around P(1)				
P(1)	O(2i)	O(3i)	O(6e)	O(9e)
O(2i)	1.6126(5)	100.5(9)	107.8(1)	109.7(7)
O(3i)	2.4804(3)	1.6065(6)	106.9(7)	108.7(6)
O(6e)	2.4983(3)	2.4803(1)	1.4795(3)	120.9(4)
O(9e)	2.5254(9)	2.5046(5)	2.5662(1)	1.4708(8)
Tetrahedron around P(2)				
P(2)	O(1i)	O(2i)	P(2)	O(1i)
O(1i)	1.6120(2)	100.7(7)	107.4(8)	109.7(3)
O(2i)	2.4853(7)	1.6164(2)	107.3(7)	108.6(1)
O(7e)	2.4843(1)	2.4879(6)	1.4650(7)	120.7(8)
O(8e)	2.5346(1)	2.5175(5)	2.5637(8)	1.4838(6)
Tetrahedron around P(3)				
P(3)	(O1i)	(O3i)	(O4e)	(O5e)
O(1i)	1.6058(7)	101.4(4)	107.8(7)	111.2(4)
O(3i)	2.4836(6)	1.6045(7)	107.4(7)	110.5(9)
O(4e)	2.4914(1)	2.48390	1.4762(3)	117.3(4)
O(5e)	2.5386(2)	2.5308(4)	2.5158(1)	1.4705(7)
P(1)–P(2)	2.8773(2)	P(2)–O(1i)–P(3)	129.4(1)	
P(1)–P(3)	2.9289(6)	P(1)–O(2i)–P(3)	131.6(6)	
P(2)–P(3)	2.9081(6)	P(1)–O(3i)–P(2)	125.8(9)	
P(2)–P(1)–P(3)	60.2(1)			
P(1)–P(2)–P(3)	60.7(2)			
P(1)–P(3)–P(2)	59.1(6)			

Table 4. Main interatomic distances (A°) and bond angles (°) in the P_3O_9 ring [8].

3.3. Characterization by infrared spectroscopy

Crystals were ground in a mortar with dry KBr powder in a ratio of 2:200 and pelleted in a press ($8*10^3$ kg, 30 s). Then, they were stored at 95°C for 1 d to dry before use.

The IR spectrum of $BaCsP_3O_9.2H_2O$ illustrated in **Figure 4** reveals the presence of three bands due to water molecules in the domain 4000–1600 cm^{-1}. This confirms the existence of nonequivalent positions of water molecules in the $BaCsP_3O_9.2H_2O$ atomic arrangement: 3449 cm^{-1} attributed to O-H valence vibration, around 3270 cm^{-1} to hydrogen bonds and 1637 cm^{-1} to δHOH deformation. The valence vibration bands related to the P_3O_9 cycles are expected in the domain 1400–650 cm^{-1}, as well as possible bands due to interactions between P_3O_9 cycles and water molecules and also of water vibration modes.

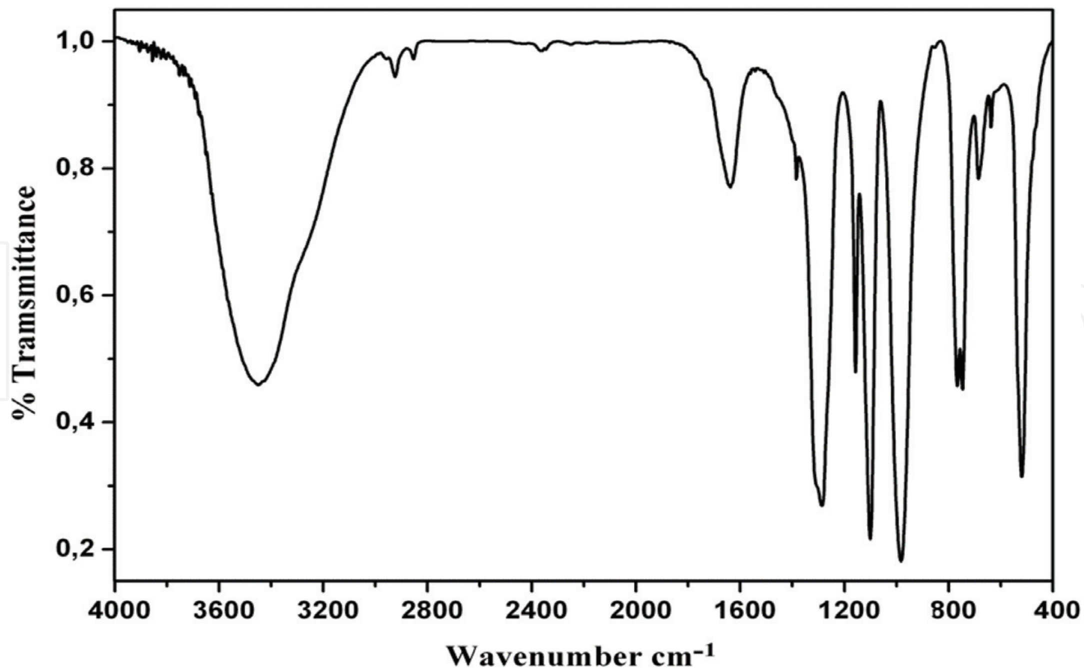

Figure 4. FTIR spectrum of $BaCsP_3O_9.2H_2O$ crystal.

The vibration modes of the phosphate anions usually occur in the 1400–650 cm^{-1} area. The two IR bands observed at 1384 and 1286 cm^{-1} can be attributed to the νas (PO_2) stretching vibration (**Table 5**). The shouldered band at 1157 cm^{-1} and the doublet observed at 1100 and

ν (cm^{-1})	Vibration
3449	ν OH
1637	
	δ HOH
1637	
1384	ν_{as} OPO^-
1286	
1157	ν_s OPO^-
1100	
983	ν_{as} POP
767	ν_s POP
747	
685	
	δ OPO^-
637	+
519	ρ OPO^-

Table 5. Frequencies (cm^{-1}) of IR absorption bands for $BaCsP_2O_9.2H_2O$.

983 cm^{-1} can be assigned to νs(PO_2) and νas(POP), respectively. The most characteristic feature of the P_3O_9 ring anions is the occurrence of a strong intensity band near 767 cm^{-1} in addition to 747 cm^{-1} due to the νs(POP) stretching vibration. The weak peak appearing at 685 cm^{-1} can be assigned to νs(POP) [9]. The broad bands observed at 519 cm^{-1} and the weak peak at 637 cm^{-1} can be due to the deformation vibrations of the anionic group.

In the spectral domain 650–400 cm^{-1}, the spectrum of $BaCsP_3O_9.2H_2O$ (**Figure 4**) shows bending vibration band characteristic of phosphates with ring anions.

4. Vibrational study

The percentage of participation of each group was determined (**Table 6**). The geometrical parameters of the P3O9 3-ring with D3h symmetry, optimized by the MNDO [10] programs, are comparable with those obtained, by X-ray diffraction for the compounds with known structures.

$^{31}P_3{}^{16}O_9{}^{3-}$	$^{31}P_3{}^{18}Oi_3{}^{16}Oe_6{}^{3-}$		$^{33}P_3{}^{16}O_9{}^{3-}$		$^{31}P_3{}^{16}Oi_3{}^{18}Oe_6{}^{3-}$		% of participation
ν(cm^{-1})	ν (cm^{-1})	Δν (cm^{-1})	ν (cm^{-1})	Δν (cm^{-1})	ν (cm^{-1})	Δν cm^{-1})	
1287.75	1287.52	0.23	1269.04	18.71	1249.67	38.08	
1271.80	1271.77	0.03	1253.83	17.97	1233.02	38.78	$\nu_{as}PO_2$ (99)
1271.79	1271.76	0.03	1253.81	17.98	1233.01	38.78	$\nu_{as}PO_2$ (100)
1225.00	1179.05	45.95	1215.39	9.61	1223.98	1.02	$\nu_{as}POP$ (98) + υ_sPO_2 (2)
1224.94	1178.99	45.95	1215.23	9.71	1223.92	1.02	υ_sPO_2 (100)
1168.89	1168.79	0.10	1156.02	12.87	1127.56	41.33	
1108.24	1098.42	9.82	1102.00	6.24	1062.75	45.49	$\nu_{as}POP$ (18) + υ_sPO_2 (82)
1108.21	1098.39	9.82	1101.97	6.24	1062.72	45.49	υ_{as} POP (100)
1059.25	1011.03	48.22	1052.97	6.28	1059.01	0.24	
780.69	768.59	12.10	765.37	15.32	776.16	4.53	υ_sPOP (73) + δPO_2 (27)
780.68	768.57	12.11	765.37	15.31	776.14	4.54	
670.86	659.43	11.43	663.10	7.76	660.19	10.67	υ_sPOP (52) + δPO_2 (48)
558.95	536.78	22.17	555.05	3.90	552.77	6.18	γPOP (60) + γ_RPO_2 (40)
511.25	495.99	15.26	509.05	2.20	501.27	9.98	δPOP (δcycle) (78)
436.70	433.13	3.57	432.42	4.28	422.94	13.76	
436.68	433.11	3.57	432.41	4.27	422.92	13.76	δPOP (21) + δPO_2 (79)
420.07	417.52	2.55	413.15	6.92	411.17	8.90	γ_wPO_2 (78)
418.47	406.18	12.29	416.87	1.60	410.01	8.46	γPOP (59) + γ_TPO_2 (41)
418.41	406.12	12.29	416.81	1.60	409.96	8.45	
301.96	301.61	0.35	301.36	0.60	285.89	16.07	δPO_2 (98)
298.71	292.63	6.08	298.22	0.49	289.41	9.30	δPOP(40) + γ_wPO_2 (60)
298.67	292.59	6.08	298.18	0.49	289.37	9.30	
280.95	279.15	1.80	279.08	1.87	269.77	11.18	γPOP (14) + γ_TPO_2 (86)
280.92	279.11	1.81	279.05	1.87	269.74	11.18	
256.50	253.00	3.50	255.02	1.48	246.50	10.00	δPOP (26) + γ_w PO_2 (74)
256.49	252.98	3.51	255.01	1.48	246.49	10.00	γ_TPO_2 (100)
214.13	214.13	0.00	214.13	0.00	201.88	12.25	
49.08	48.30	0.78	49.08	0.00	47.01	2.07	γPOP (27) + γ_RPO_2 (73)
35.78	35.11	0.67	35.77	0.01	34.39	1.39	
34.40	33.75	0.65	34.40	0.00	33.00	1.40	γPOP (33) + γ_RPO_2 (67)

Table 6. IR frequencies and displacements (Δν in cm^{-1}) calculated for the P_3O_9 (D_{3h} symmetry).

All the Raman spectra available in the literature of compounds with the $P_3O_9^{3-}$ cycle of C_{3h} symmetry, in $LnP_3O_9.3H_2O$ [11] and $M^{II}M^{I}P_3O_9$ with benitoite structure 4, and cycle of Cs symmetry in $NiRb_4(P_3O_9)_2.6H_2O$ [17, 18], $ZnM^{I}{}_4(P_3O_9)_2.6H_2O$ (M^I = K, Rb) [12, 13], $M^{II}K_4(P_3O_9)_2.7H_2O$ (M^{II} = Ni,Co), C_1 in $M^{II}(NH_4)_4(P_3O_9)_2.4H_2O$ (M^{II} = Cu, Co, Ni) [14], and $NiNa_4(P_3O_9)_2.6H_2O$ [15] are characterized by three intense bands situated between 1153 and 1180, 640–680, and 297–313 cm^{-1}, which confirm the results of our calculations (**Table 6**). Indeed, the theory predicts on the whole four bands with A'_1 modes for the P_3O_9 ring with D_{3h} symmetry which are situated, according to our results, at 1169 cm^{-1} for νs P-Oe, 671 cm^{-1} for δs P-Oi, 559 cm^{-1} for δsPOiP, and 302 cm^{-1} for δs PO_2. These four frequencies are predicted to be characteristic in any Raman spectrum of a cyclotriphosphate (with cycle of symmetry, C_3, C_2, Cs, or C_1). These four IR fundamental frequencies have a null calculated intensity and are non-observable for D_{3h} or C_{3h} symmetries, and their appearance in any IR spectrum indicates a symmetry lower than C_{3h}.

M. G.			Δν (cm^{-1})			ν (cm^{-1}) in $BaCsP_3O_9.2H_2O$		
D_{3h}νcal (cm^{-1})	I/Imax	Mode (IR, Ra)				Mode (IR, Ra)		Movement
1287.75	55.3	E "(-,+)	0.23	18.71	38.80	A(+,+)	1297	$ν_{as}$ PO_2
								$ν_{as}PO_2$
1271.80	0.00		0.03	17.97	38.78	A(+,+)	1274	$ν_{as}$ PO_2
		E '(+,+)						
1271.79	0.00		0.03	17.98	38.78	A(+,+)	1269	
							1211	
		A'1(-,+)						$ν_{as}POP$
1225.00	100		45.95	9.61	1.02	A(+,+)		
1224.94	100	E '(+,+)	45.95	9.71	1.02	A(+,+)		$ν_{as}$ POP
1168.89	0.00	A'2(-,-)	0.10	12.87	41.33	A(+,+)	1166	$ν_s$ PO_2
								$ν_sPO_2$
1108.24	5.85	E '(+,+)	9.82	6.24	45.49	A(+,+)	1117	
1108.21	5.85		9.82	6.24	45.49	A(+,+)	1103	$ν_s$ PO_2
		A'1(-,+)						
1059.25	0.00		48.22	6.28	0.24	A(+,+)	977	
							880	vasPOP
								combination
780.69	18.35		12.10	15.32	4.53	A(+,+)	760	
780.68	18.35		12.11	15.32	4.54	A(+,+)	743	$ν_sPOP$
								$ν_sPOP$
670.86	0.00		11.43	7.76	10.67	A(+,+)	670	

Δν(cm^{-1}): effect of the isotopic substitution; Δν(cm^{-1}): difference between the calculated Value of the frequency before and after the substitution; M. G: molecular group.

Table 7. Attribution of the observed valence IR frequencies (cm^{-1}) of the P_3O_9 ring (C_1) in $BaCsP_3O_9.2H_2O$.

This allowed us an attribution of the 30 fundamental frequencies of the cycle D_{3h} on valid theoretical bases including 12 valence vibration frequencies and 18 bending vibration frequencies. The correlation between the D_{3h} group and the site group C_1 shows that the simple normal modes (A'_1, A'_2, A''_1, and A''_2), of the D_{3h} group, are resolved each into the mode A of the C_1 group and the doubly degenerate E′ and E″ modes are resolved into two modes and are active in IR and Raman. The factor group analysis predicts for four cycles of the unit cells of $BaCsP_3O_9.2H_2O$ (C_{2h}), respectively, 24 and 36 valence vibration bands active in IR. But, we observe in the IR spectra of $BaCsP_3O_9.2H_2O$ (C_{2h}) only six or seven bands and one inflection (**Figure 4**). It seems that the vibrational couplings between the P_3O_9 cycles of the unit cell are absent or very weak; thus, we will be able to interpret the IR spectrum, in the range 1400–650 cm^{-1}, of $BaCsP_3O_9.2H_2O$ according to the vibrations of an isolated cycle with local symmetry C_1. The values of the calculated frequencies, for the D_{3h} symmetry, are close to those observed for $BaCsP_3O_9.2H_2O$ (**Table 6**). **Table 7** gives the attribution of the observed valence frequencies, 1400–650 cm^{-1}, of the P_3O_9 ring, with D_{3h} symmetry of $BaCsP_3O_9.2H_2O$.

5. Thermal analysis

The curve corresponding to the TG analyses in an air atmosphere and at a heating rate of 10°C.min^{-1} of BaCsP3O9.2H2O is given in **Figure 5**. The dehydration of the barium cyclotriphosphate and of cesium dihydrate BaCsP3O9.2H2O is carried out in two steps in two temperature ranges from 105 to 180°C and from 180 to 580°C (**Figure 5**). In the thermogravimetric (TG) curve, the first step between 95 and 180°C corresponds to the elimination of 1.14 water molecules; the second step from 180 to 580°C is due to the removal of 0.86 water molecules.

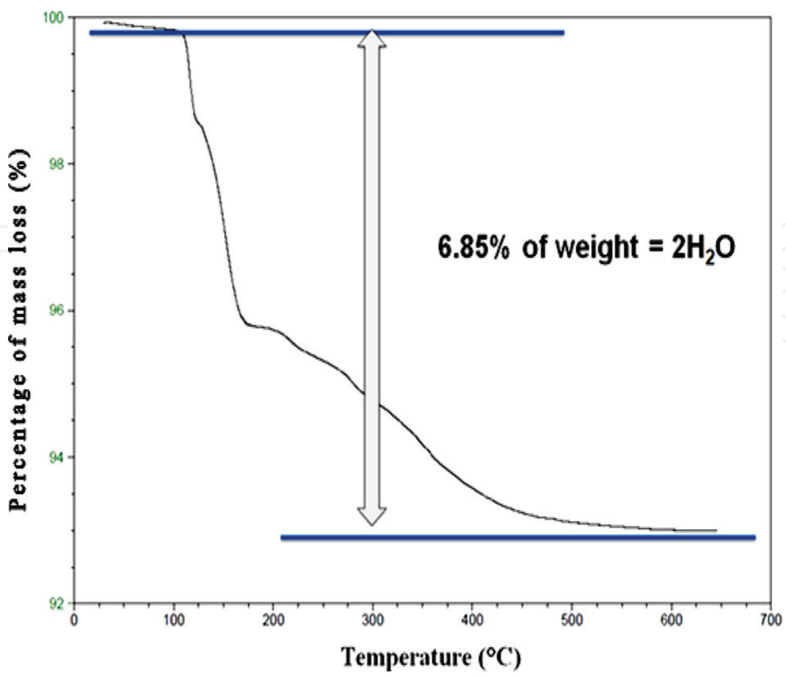

Figure 5. TG curves of $BaCsP_3O_9.2H_2O$ at rising temperature (10°C min^{-1}).

6. Comparison of the thermal behavior of $BaCsP_3O_9.2H_2O$ with $BaNH_4P_3O_9.2H_2O$ and $BaTlP_3O_9.2H_2O$

The thermal behavior of $BaNH_4P_3O_9.2H_2O$ and $BaTlP_3O_9.2H_2O$ [16] was studied (Laboratory of Physical Chemistry of Materials, Ben M'sik faculty of Sciences, Casablanca, Morocco). It would be useful to compare the thermal behavior of $BaCsP_3O_9.2H_2O$ with that of its isotypic compounds $BaNH_4P_3O_9.2H_2O$ and $BaTlP_3O_9.2H_2O$.

The thermal behavior of $BaCsP_3O_9.2H_2O$ is different from that obtained in the case of $BaTlP_3O_9.2H_2O$ [16], which leads to the anhydrous barium and thallium $BaTlP_3O_9$ cyclotriphosphate at 280°C. After amorphous X-ray state, $BaTlP_3O_9$ remains stable till its melting point at 670°C.

$$BaTlP_3O_9.2H_2O \xrightarrow{70-270^\circ C} Amorphous\ X-ray\ \mathrm{Phase} + 2H_2O \xrightarrow{300^\circ C} BaTlP_3O_9$$

The total dehydration of $BaCsP_3O_9.2H_2O$, after passing through an amorphous X-ray state, leads to monobarium polyphosphate and tetracerium $BaCs_4(PO_3)_6$ at 500°C [17, 18].

$$BaCsP_3O_9.2H_2O \xrightarrow{100-250^\circ C} Amorphous\ X-ray\ Phase + 2H_2O \xrightarrow{450^\circ C} ¼\ BaCs_4(PO_3)_6\ crystallized$$
$$+ ¾\ \left[Ba(PO_3)_2\right]\infty(BaP_2O_6 amorphous\ in\ X-ray\ diffraction).$$

7. Conclusion

The cyclotriphosphate $BaCsP_3O_9.2H_2O$ was obtained as a monocrystal by the resin exchange method. It crystallizes in the monoclinic system, space group $P2_1/n$, Z = 4, and is an isotype of $BaNH_4P_3O_9.2H_2O$ and $BaTlP_3O_9.2H_2O$.

The crystal structure of $BaCsP_3O_9.2H_2O$ was solved from 2448 independent reflections. The final value of the unweighted reliability factor is R = 0.0329. The unit cell of $BaCsP_3O_9.2H_2O$ contains four $P_3O_9^{3-}$ rings, each of them consists of three crystallographically independent P (1)O4, P(2)O4, and P(3)O4 tetrahedra. The three tetrahedra have no special characteristics. The P_3O_9 cycle observed in the structure of $BaCsP_3O_9.2H_2O$ has no internal symmetry. The cohesion between the cycles $P_3O_9^{3-}$ is ensured via the associated cations Cs^+ and Ba^{2+}. The main geometrical characteristics of the three P(1)O4, P(2)O4, and P(3)O4 tetrahedra of the P_3O_9 cycle are quite similar to those observed generally in cyclotriphosphates.

The thermogram (TG) of $BaCsP_3O_9.2H_2O$ shows that dehydration takes place in two distinct steps between 70 and 560°C.

The total removal of the water at 560°C is accompanied by a total destruction of the $BaCsP_3O_9.2H_2O$ structure, probably leading to a mixture of amorphous oxidesin X-ray diffraction BaO + 3/2 P_2O_5 + ½ Cs_2O. The product resulting from calcinations of $BaCsP_3O_9.2H_2O$ between 300 and 560°C is the long chain polyphosphate $BaCs_4(PO_3)_6$.

Author details

Soufiane Zerraf[1]*, Mustafa Belhabra[1], Aziz Kheireddine[1], Malika Tridane[1,2], Hicham Moutaabbid[3], Mohammed Moutaabbid[1] and Said Belaaouad[1]

*Address all correspondence to: soufiane.zerraf@gmail.com

1 Laboratory of Physical Chemistry of Materials, Ben M'sik Faculty of Sciences, Casablanca, Morocco

2 Regional Center for Education and Training Occupations Casablanca Anfa, Bd Bir Anzarane Casablanca, Morocco

3 Institute of Mineralogy, Physics of Materials, and Cosmochemistry (IMPMC) Sorbonne Universities—UPMC University Paris, Cedex, France

References

[1] Kheireddine A, Tridane M, Belaaouad S. Powder Diffraction. 2012;**27**:32-35. DOI: 10.13171/mjc.2.4.2013.22.05.12

[2] Masse R, Averbuch-Pouchot MT. Materials Research Bulletin. 1977;**12**:13-16. DOI: 10.1016/0025-5408(77)90083-6

[3] Simonot-Grange MH. Journal of Solid State Chemistry. 1983;**46**:76-86. DOI: 10.1016/0022-4596(83)90128-7

[4] Durif A. Crystal Chemistry of Condensed Phosphates. New York: Plenum Press; 1995. ISBN 978-1-4757-9894-4

[5] Sheldrick GM. Acta Crystallographica. 2008;**64**:112-122. DOI: 10.1107/S0108767307043930

[6] Dolomanov OV, Bourhis LJ, Gildea RJ, Howard JA, Puschmann H. Journal of Applied Crystallography. 2009;**42**:339-341. DOI: 10.1107/S0021889808042726

[7] Tarte P, Rulmont A, Sbai K, Simonot-Grange MH. Spectrochimica Acta. 1987;**43A**:337-345. DOI: 10.1016/0584-8539(87)80114-9

[8] Zerraf S, Belhabra M, Kheireddine A, Lamsatfi R, Tridane M, Moutaabbid H, Baptisteb B, Moutaabbid M, Belaaouad S. Phosphorus Sulfur Silicon and the Related Elements. 2017;**192**:1286-1293. DOI: 10.1080/10426507.2017.1333507

[9] Tace EM, Charaf A, Fahim I, Moutaabbid M, Kheïreddine A, Ouaalla F-E, et al. Phosphorus, Sulfur and Silicon and the Related Elements. 2011;**186**:1501-1514. DOI: 10.1080/10426507.2010.520173

[10] Dewar MJS, Thiel W. Journal of the American Chemical Society. 1977;**99**:4899-4902. DOI: 10.1021/ja 00457a004

[11] Sbai K, Abouimrane A, Lahmidi A, El Kababi K, Hliwa M, Vilminot S. Annales de Chimie Science des Materiaux. 1999;**25**(supp. 1):139-143

[12] Abouimrane A. Thèse de Doctorat. Casablanca, Maroc; 2000

[13] Abouimrane A, Sbai K, El Kababi K, Lahmidi A, Atibi A, Vilminot S. Phosphorus, Sulfur and Silicon and the Related Elements. 2001;**179**:69-83

[14] Sbai K, Abouimrane A, El Kababi K, Vilminot S. Journal of Thermal Analysis and Calorimetry. 2002;**68**:109-122. DOI: 10.1023/A:10149288

[15] Sbai K, Atibi A, Charaf A, Radid M, Jouini A. Annales de Chimie Science des Materiaux. 2001;**26**:45-61

[16] Belaaouad S, Sbai KJ. Journal of Physics and Chemistry of Solids. 2003;**64**:981-991. DOI: 10.1016/S0022-3697(02)00461-4

[17] Averbuch-Pouchot MT, Durif A. Acta Crystallographica. 1986;**C42**:928-930. DOI: 10.1107/S0108270186093976

[18] Belhabra M, Kheireddine A, Moutaabbid H, Baptiste B, Lamsatfi R, Fahim I, et al. Research Journal of Recent Sciences. 2015;**6**(Issue 12):7832-7836. ISSN: 0976-3031